The free escape continuum of diffuse ions upstream of the Earth's quasi-parallel bow shock

K. J. Trattner,[1] F. Allegrini,[2,3] M. A. Dayeh,[2] H. O. Funsten,[4] S. A. Fuselier,[2] D. Heirtzler,[5] P. Janzen,[6] H. Kucharek,[5] D. J. McComas,[2,3] E. Möbius,[5] T. E. Moore,[7] S. M. Petrinec,[1] D. B. Reisenfeld,[6] N. A. Schwadron,[5] and P. Wurz[8]

Received 29 October 2012; revised 29 May 2013; accepted 6 July 2013; published 29 July 2013.

[1] The Earth's bow shock is very efficient in accelerating ions out of the incident solar wind distribution to high energies (≈ 200 keV/*e*). Fluxes of energetic ions accelerated at the quasi-parallel bow shock, also known as diffuse ions, are best represented by exponential spectra in energy/charge, which require additional assumptions to be incorporated into these model spectra. One of these assumptions is a so-called "free escape boundary" along the interplanetary magnetic field into the upstream direction. Locations along the IBEX orbit are ideally suited for in situ measurements to investigate the existence of an upstream free escape boundary for bow shock accelerated ions. In this study we use 2 years of ion measurements from the background monitor on the IBEX spacecraft, supported by ACE solar wind observations. The IBEX Background Monitor is sensitive to protons > 14 keV, which includes the energy of the maximum flux for diffuse ions. With increasing distance from the bow shock along the interplanetary magnetic field, the count rates for diffuse ions stay constant for ions streaming away from the bow shock, while count rates for diffuse ions streaming toward the shock gradually decrease from a maximum value to ~1/*e* at distances of about 10 R_E to 14 R_E. These observations of a gradual decrease support the transition to a free escape continuum for ions of energy >14 keV at distances from 10 R_E to 14 R_E from the bow shock.

Citation: Trattner, K. J., et al. (2013), The free escape continuum of diffuse ions upstream of the Earth's quasi-parallel bow shock, *J. Geophys. Res. Space Physics*, *118*, 4425–4434, doi:10.1002/jgra.50447.

1. Introduction

[2] Energetic ions with energies from just above the solar wind energy of 1 to about 200 keV/*e* upstream of the Earth's bow shock have been studied for several decades since first reported by *Asbridge et al.* [1968] and *Lin et al.* [1974] based on VELA and IMP 6 measurements, respectively. These bow shock associated energetic ions consist of several different distributions, which were originally identified as the reflected and the diffuse components [e.g., *Gosling et al.*, 1978; *Paschmann et al.*, 1981]. At times also, the intermediate state of the two components can be observed [*Paschmann et al.*, 1981].

[3] The reflected component is associated with the quasi-perpendicular bow shock for which the angle between the shock normal and the direction of the interplanetary magnetic field (IMF) $\Theta_{Bn} > 45°$. The reflected component is defined as a beamlike distribution, which streams away from the bow shock along the magnetic field lines against the incoming solar wind.

[4] *Greenstadt* [1976] demonstrated that the diffuse component is only observed for $\Theta_{Bn} < 45°$, the quasi-parallel bow shock. The diffuse component is generally more isotropic and moves along the IMF in the upstream direction while the field is convecting downstream with the solar wind. At energies > 30 keV, the bow shock related ions in general belong to the high-energy tail of the diffuse ion component [*Scholer et al.*, 1980a]. The reflected and diffuse ion components each have a number density *N* of about 1% of the solar wind density [*Bonifazi and Moreno*, 1981].

[5] Considerable evidence has been accumulated as early as the ISEE mission that below 200 keV, the bow shock itself is the dominant source of energetic ions [e.g., *Gosling et al.*, 1978; *Paschmann et al.*, 1981], while observations of upstream energetic ions > 300 keV/*e* are of magnetospheric origin [e.g., *Sarris et al.*, 1976, 1978; *Krimigis et al.*,

[1]Lockheed Martin Advanced Technology Center, Palo Alto, California, USA.
[2]Southwest Research Institute, San Antonio, Texas, USA.
[3]Department of Physics and Astronomy, University of Texas, San Antonio, Texas, USA.
[4]Los Alamos National Laboratory, Los Alamos, New Mexico, USA.
[5]Institute for the Study of Earth, Oceans, and Space, University of New Hampshire, Durham, New Hampshire, USA.
[6]Department of Physics and Astronomy, University of Montana, Missoula, Montana, USA.
[7]Heliophysics Science Division, NASA Goddard Space Flight Center, Greenbelt, Maryland, USA.
[8]Physics Institute, University of Bern, Bern, Switzerland.

Corresponding author: K. J. Trattner, Lockheed Martin Advanced Technology Center, 3251 Hanover St., Palo Alto, CA 94304, USA. (trattner@spasci.com)

2169-9380/13/10.1002/jgra.50447

1978]. Generally, the energetic particles in the upstream region are accompanied by hydromagnetic waves in the general frequency regime 0.01–0.3 Hz [e.g., *Fairfield*, 1969; *Hoppe et al*., 1981]. The waves are thought to constitute scattering centers for the ions, which provide for diffusive transport and Fermi acceleration at the bow shock [e.g., *Axford et al*., 1977]. *Lee* [1982] explicitly included the excitation of hydromagnetic waves by the energetic ion population in his self-consistent model of the wave-particle interaction. This model has been successfully tested with observations from the Active Magnetospheric Particle Tracer Explorers (AMPTE)/Ion Release Module (IRM) satellite [e.g., *Möbius et al*., 1987; *Trattner et al*., 1994; *Gordon et al*., 1999].

[6] Many observed features of the diffuse ions, such as their general directional distributions, spectra, and spatial distribution in front of the bow shock, have been successfully interpreted within models based on diffusive acceleration [e.g., *Ipavich et al*., 1981a; *Scholer et al*., 1980a, 1981, 1989; *Trattner et al*., 1994].

[7] A significant property of diffuse ions observed at the Earth's bow shock is the deviation of the differential energy spectrum from a simple power law. Beyond 30 keV/*e*, the diffuse ion energy spectra are characterized by an exponential function in energy per charge [e.g., *Ipavich et al*., 1981a]. To describe the features such as the exponential spectra in the energy per charge, additional assumptions had to be included in the models. For example, ion loss across a free escape boundary along the interplanetary magnetic field into the upstream direction [e.g., *Ellison*, 1981; *Lee et al*., 1981] or loss by diffusion perpendicular to the magnetic field [e.g., *Lee*, 1982] has been assumed. Other alternatives to explain the spectral shape include a finite time of connection with the bow shock [*Scholer et al*., 1980a; *Forman and Drury*, 1983] or the contribution of shock drift acceleration to the energization [*Jokipii*, 1982].

[8] The concept of a free escape boundary upstream of the Earth's bow shock is thought to result from a limitation of the upstream wavefield to a region close to the shock. The behavior that can be described by a free escape boundary is due to the decay of wave activity upstream of the shock. Ions, which cross this upstream boundary, can leave the shock vicinity and are not scattered back downstream. This idea was developed from simultaneous observations of energetic ions at ISEE 3 more than 200 R_E upstream and ISEE 1 close to the quasi-parallel bow shock, respectively. For these observations, both satellites were magnetically connected with the quasi-parallel bow shock. Close to the bow shock, the ion distribution was more or less isotropic, indicating strong scattering of the ions in the upstream wavefield, while far upstream, the ion distribution was only outward streaming, indicating essentially scatter-free motion away from the bow shock [*Scholer et al*., 1980b].

[9] Previous satellite missions upstream of the Earth's bow shock were either too close to the bow shock (e.g., Cluster and Geotail) or too far away (e.g., ISEE 3) for the in situ measurements needed to investigate this free escape boundary where energetic ions become decoupled from the upstream wavefield. The IBEX spacecraft [*McComas et al*., 2009a] was launched into a near equatorial orbit with an ~18,000 km perigee by ~50 R_E apogee orbit with a ~7.5 day period, which provides extended periods of time in the region upstream of the bow shock and is ideal to investigate this free escape boundary. While the main mission of the IBEX satellite has been the first global images of the heliosphere's interaction with the local interstellar medium through observations of energetic neutral atoms [*McComas et al*., 2009b], its background monitor measures the in situ flux and covers the energy range required for studying energetic ions at the Earth's bow shock. This investigation reveals a gradual decrease in the measured count rate for energetic diffuse ions scattered back to the bow shock at a distance of ~15 R_E from the shock.

2. Instrumentation

[10] The data used in this study come from the IBEX Background Monitor (IBaM) [*Allegrini et al*., 2009] onboard the IBEX satellite. IBaM quantifies the in situ energetic ion background environment by making an integral measurement of >~14 keV protons in a 7° FWHM field of view (FOV) aligned with the IBEX-Hi energetic neutral atom (ENA) imager viewing direction [*Funsten et al*., 2009]. The IBaM uses a relatively simple detection method in which ions enter a collimator that defines the FOV, pass through two thick carbon foils if they have sufficient energy, and are detected by a channel electron multiplier. The combined thickness of the two foils sets a minimum proton energy threshold of ~14 keV. The thick foils also block a large fraction of UV light that might be observed in the FOV. Exceptions are the strong sources of UV emissions such as the brightest UV emission from the Earth's geocorona and astrophysical X-ray sources such as Sco X1.

[11] The IBaM was designed to measure energetic ions (e.g., foreshock and magnetospheric ions) that have a high enough energy to successfully pass through the electrostatic potentials in the IBEX collimators and produce elevated backgrounds in the IBEX ENA imagers [*Wurz et al*., 2009]. For the typical upstream diffuse ion spectra as discussed in *Ipavich et al*. [1981b] and *Trattner et al*. [1994], IBaM's response peaks between 20 and 30 keV with a width of ~90 keV. This response peak is expected to move gradually to higher energies with increasing distance from the bow shock, in agreement with predictions from the diffuse acceleration theory [*Lee*, 1982]. IBEX is a nearly Sun-pointing spinning spacecraft with sensor look directions perpendicular to the spin axis. IBaM integrates counts over a ~7° swath in the sky and creates a 60-bin histogram every 3 min, with the first bin centered on the north ecliptic pole.

[12] Solar wind context measurements are provided by the ACE Solar Wind Experiment [*McComas et al*., 1998] and the ACE Magnetic Field Instrument [*Smith et al*., 1998]. All solar wind and IMF data are available at CDAWeb.

3. Observations

[13] The IBaM data set discussed in this study covers the time period from 10 December 2008 to 3 October 2010 at 3 min resolution with the associated time stamp centered on each sample. The solar wind and IMF observations at ACE are propagated to the bow shock using the ACE-measured solar wind speed. The resulting solar wind time series are 6 min averages centered on the 3 min IBEX time stamps. For each of the 3 min data samples, we subsequently calculate the distance between the IBEX satellite and a model bow shock along the (convected) IMF as well as the angle

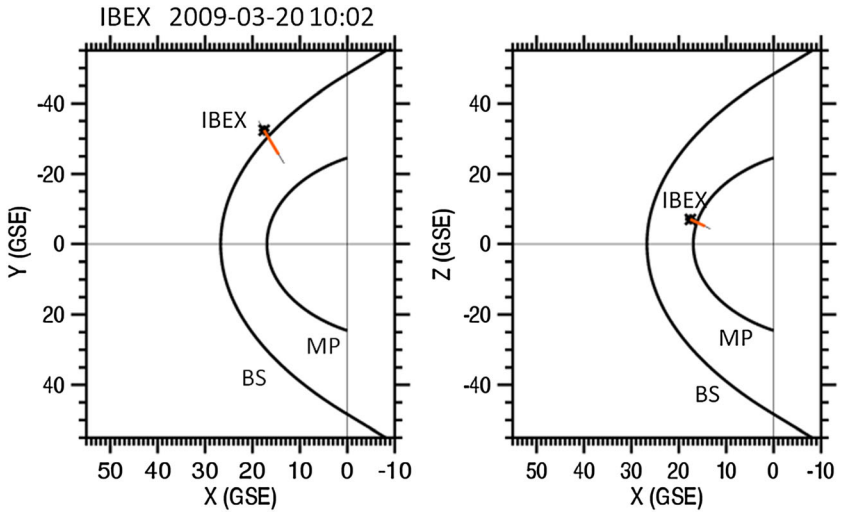

Figure 1. The location of the IBEX satellite in front of the Earth's bow shock (BS) and the magnetopause (MP) on 20 March 2009. The line connecting the satellite with the bow shock represents the direction of the IMF observed by the ACE satellite during the observation time. The IMF data are convected to the BS position. The red section of the IMF line highlights the distance from IBEX to the BS along the magnetic field direction used in the study.

between the IMF direction and the shock normal (Θ_{Bn}) at the intersection point between the IMF line and the bow shock. For times when IBEX is not magnetically connected to the model bow shock, we record the minimum distance between the magnetic field line passing through IBEX and a line parallel to the IMF and tangent to the shock surface.

[14] Figure 1 shows the IBEX location on 20 March 2009 at 10:02 UT in the dawn sector upstream of the Earth's bow shock. The bow shock and the magnetopause locations are derived from the *Farris and Russell* [1994] bow shock model and the *Petrinec and Russell* [1996] magnetopause model, respectively, using the convected solar wind and IMF observations from the ACE satellite. The solar wind density, N_{SW}, for this time was about 0.5 cm^{-3} with a solar wind velocity, V, of about 313 km/s. The IMF direction was relatively steady for hours prior to this time with (−2, 4.4, −1.3) [nT] for B_X, B_Y, and B_Z in GSE coordinates, respectively.

[15] The IBEX satellite is located on the dawnside of the bow shock at (17.52, −32.37, 7.01) R_E for X, Y, and Z in GSE coordinates, respectively. The thin black line drawn through the IBEX position in Figure 1 represents the convected IMF direction observed by the ACE satellite, while

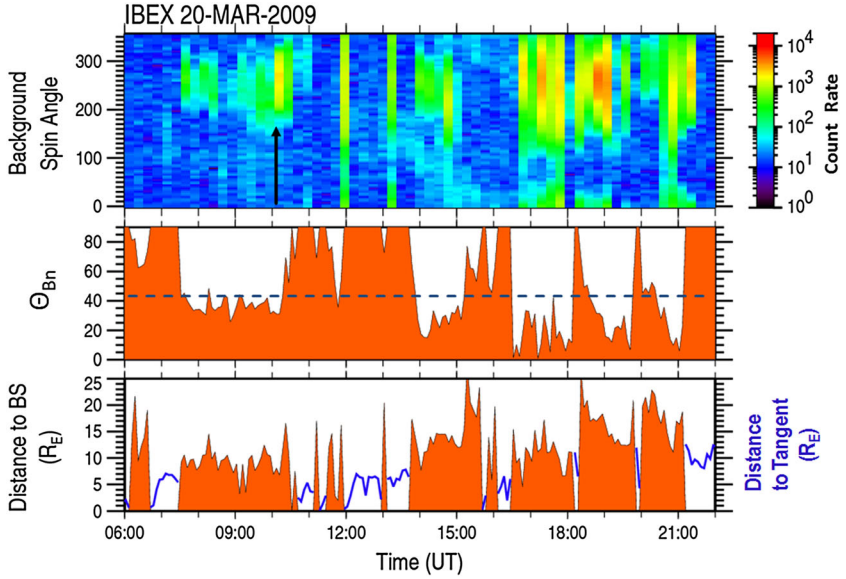

Figure 2. (top) The IBEX Background Monitor count rate, (middle) the angle between the shock normal and the IMF Θ_{Bn}, and (bottom) the distance to the bow shock. The blue line in the bottom panel represents the minimum distance between the magnetic field line passing through IBEX and a line parallel to the IMF and tangent to the shock surface, for times when the magnetic field at IBEX is not connected to the bow shock. The black arrow in the top panel marks an event time (10:02 UT) discussed in Figure 3.

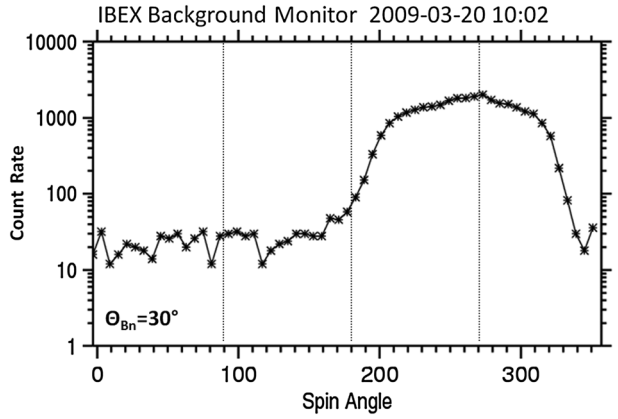

Figure 3. The IBEX Background Monitor count rate versus the spin angle at 20 March 2009, 10:02 UT. IBEX was magnetically connected to the Earth's bow shock with $\Theta_{Bn} = 30°$. The count rate reaches about 2300 for the sectors looking toward the bow shock, while the opposing sectors only reach about 20.

the red section of the line depicts the distance between the IBEX satellite and the bow shock along the direction of the IMF. The intersection point of the magnetic field line with the bow shock is located at (14.5, −25.5, 4.97) R_E in GSE coordinates and marked in Figure 1 by the termination of the red line along the IMF direction. The distance between IBEX and the bow shock along the magnetic field direction is about 7.5 R_E and these distances are used to sort the IBaM observations with respect to the model bow shock location. The angle Θ_{Bn} is calculated at the intersection point of the IMF with the bow shock and was a quasi-parallel bow shock of about 30° for this example.

[16] Figure 2 shows the time series of spin angle distributions with the IBaM count rate as a function of time (top), Θ_{Bn} (middle), and the distance of the observing satellite from the bow shock (bottom) for 20 March 2009 from about 06:00 to 22:00 UT. In this example, the IBEX data shown in this figure are from the standard IBaM data product averaged over 16 min. For the analysis below, we will use the high-resolution 3 min data set. The black arrow in Figure 2 (top) marks the time step (10:02 UT) used in the Figure 1 example for the distance and Θ_{Bn} calculation, and will be further discussed in Figure 3 below. The IBaM count rate shows regular enhancements in the spin angle sectors from about 200° to 300° throughout the entire time window. For the satellite in the dawn sector of the magnetosphere (as shown in Figure 1), this angular range looks in the direction of the bow shock and detects shock-accelerated ions emanating from the shock.

[17] Figure 2 (middle) shows that the IBaM count rate enhancements correlate remarkably well with sharp drops of Θ_{Bn} below 45° (blue dashed line), connecting the IBEX satellite to a quasi-parallel bow shock capable of generating the shock-accelerated diffuse ion population described above. The angular coverage of the diffuse ions in the IBaM expands later in the day when Θ_{Bn} dips below 25°, connecting IBEX to the core region of a quasi-parallel shock with longer connection times.

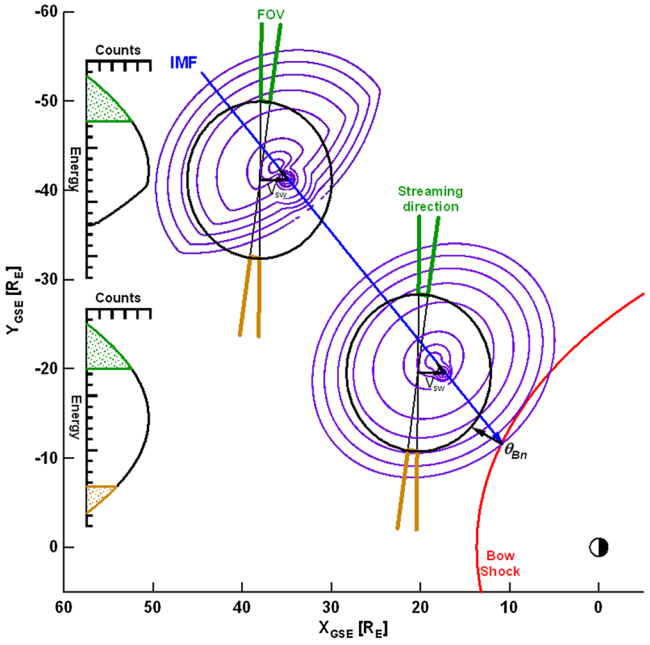

Figure 4. Schematic representation of the diffuse ion distribution upstream of the quasi-parallel shock (purple contours) with the IBEX field of view (green cones). The black circle represents the cutoff energy of the IBEX Background Monitor at about 14 keV for protons. The red line represents the bow shock and the blue arrow the upstream magnetic field direction. The left side shows spectral cuts through the diffuse ion distribution as seen by the IBEX Background Monitor. Far upstream from the quasi-parallel bow shock, the diffuse ion distribution decouples from the magnetic turbulence and streams away freely which causes a reduction in the count rate in the background monitor sectors looking away from the shock. Note that the IBEX field of view (FOV) is plotted in streaming direction to align with the diffuse ion contours.

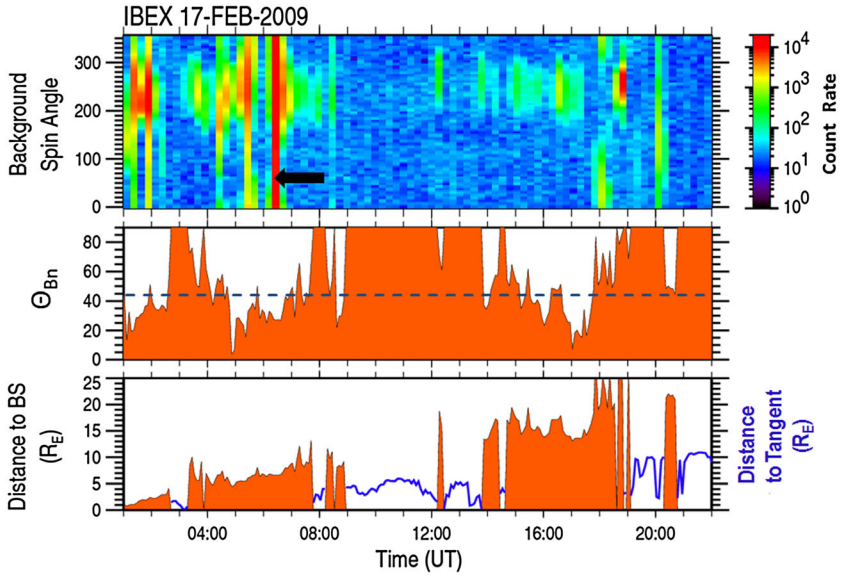

Figure 5. Same as Figure 2 but for 17 February 2009.

[18] Figure 2 (bottom) shows the distance of the IBEX satellite from the bow shock along the IMF (red solid area). The distance is around 10 R_E at the beginning of the time interval and increases to about 15 R_E toward the end of the time interval. Connection times throughout the day are interrupted by periods when the IMF rotates and IBEX no longer had a magnetic connection to the bow shock. For such times, Θ_{Bn} was set to 90° as if the satellite was connected to a perpendicular bow shock. Distinguishing actual connection times with a perpendicular bow shock from periods with no magnetic connection between the satellite and the bow shock are also depicted in Figure 2 (bottom). For disconnected intervals, the red solid area representing a magnetic connection is replaced by a blue curve showing the minimum distance between the IMF line passing through the IBEX satellite and the tangent to the bow shock, which is parallel to the IMF direction. For cases when this distance is zero, the satellite was connected to a perpendicular shock (e.g., at about 06:00 UT, 06:40 UT, 12:00 UT, and 15:40 UT).

[19] Figure 3 shows the IBaM count rate versus spin angle for a 16 min average time interval at 10:02 UT on 20 March 2009. As shown in Figure 1, at that time, IBEX was connected to a quasi-parallel bow shock with a Θ_{Bn} of about 30° at a distance of about 7.5 R_E upstream of the bow shock along the IMF direction (see also the black arrow in Figure 2). The count rate between the sectors looking toward the shock compared to the sectors looking away from the shock is dramatically different, reaching 2000 counts compared to about 20 counts, respectively.

[20] The reason for the significant difference between the count rates in different look directions is the distribution of the diffuse component itself. Diffuse ion events have been observed upstream of the bow shock for several hours. Their energy range extends from solar wind energies to 100–200 keV /*e* with a peak at about 10–20 keV /*e* [*Scholer et al*., 1979, 1981]. They show a more or less isotropic angular distribution close to the shock, which indicates the importance of wave-particle interaction processes in their acceleration. The diffuse upstream ions form a torus-shape distribution in velocity space, which moves along the magnetic field lines in the upstream direction with a bulk velocity smaller than the solar wind velocity. In the spacecraft frame, the bulk motion is directed toward the bow shock [e.g., *Paschmann et al*., 1981].

[21] A schematic representation of the diffuse ion distributions upstream of the quasi-parallel shock is shown in Figure 4. The red curve represents the location of the bow shock. The blue arrow shows the IMF direction. The black arrow at the bow shock represents the shock normal at the intersection of the magnetic field line with the bow shock, defining Θ_{Bn}. Widely spread blue contours represent the diffuse ion distribution streaming along the IMF in the upstream direction with respect to the solar wind distribution (tightly

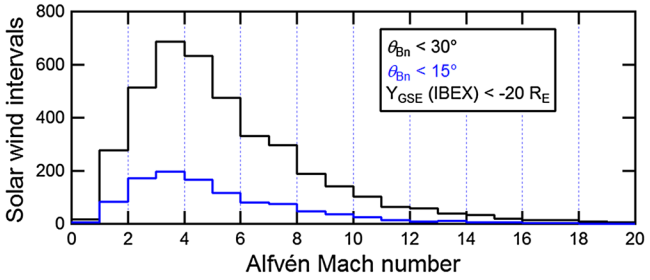

Figure 6. The Alfvén Mach number for the IBEX upstream observation intervals during the time of interest with $\Theta_{Bn} < 30°$ (black) and $\Theta_{Bn} < 15°$ (blue).

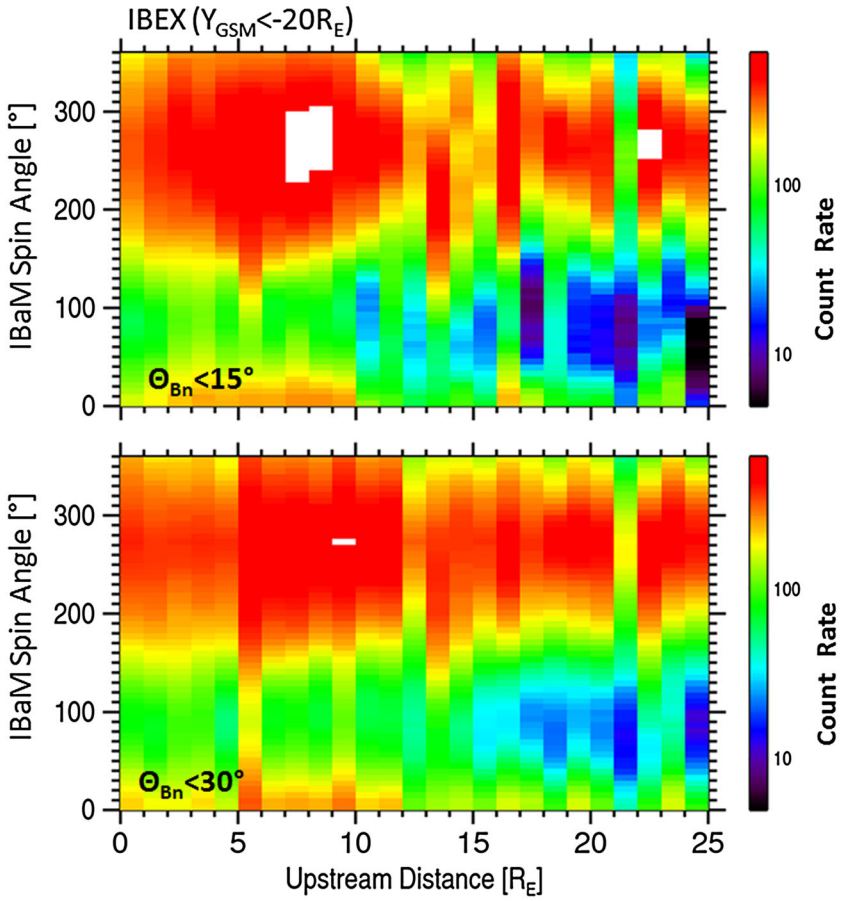

Figure 7. The spin angle of the IBEX Background Monitor versus the IBEX satellite upstream distance along the ambient magnetic field. The data considered in these panels are for IBEX locations with $Y_{GSE} < -20\,R_E$. Data subsets for (top) $\Theta_{Bn} < 15°$ and (bottom) $\Theta_{Bn} < 30°$.

spaced contours marked "SW"). In this configuration, the IBEX field of view (FOV) in the spacecraft frame is shown in green and orange shifted by V_{SW} sunward of the solar wind peak. The black circle represents the lower cutoff energy of the IBaM at 14 keV. The instrument is thus blind to everything inside that circle, which is the bulk of the diffuse ion distribution, but clearly observes the shoulders of the peak as shown. Note that the FOV is depicted in the streaming direction and not in the look direction, to be consistent with the diffuse ion contours.

[22] The left side of Figure 4 shows cuts through the diffuse ion distribution as seen by the IBaM. The unique phase space location of the diffuse ion distribution with respect to the shifted (by the solar wind speed) IBaM cutoff energy causes a significant overrepresentation of the ions streaming away from the bow shock compared to ions streaming toward the shock. This effect is clearly seen in Figures 2 and 3. Further away from the quasi-parallel bow shock (upper part of Figure 4), the diffuse ion distribution decouples from the upstream magnetic turbulence and streams freely away, which will cause a further reduction of the IBaM sectors looking away from the bow shock. The IBEX satellite is in a unique position to cross this boundary and see the decrease of the backstreaming distribution.

[23] Figure 5 shows data from 17 February 2009. The layout of Figure 5 is the same as that of Figure 2. As in the previous case, the appearance of diffuse ions in the sectors streaming away from the bow shock (Figure 5, top) correlates well with a magnetic connection of the IBEX satellite to the quasi-parallel bow shock with Θ_{Bn} below 45° (Figure 5, middle). From about 01:00 UT to about 08:00 UT, the IBEX satellite was close to and magnetically connected to the quasi-parallel bow shock (Figure 5, bottom) with the distance along the IMF increasing steadily from 0 to about $10\,R_E$. A brief interruption of this magnetic connection occurred at about 03:00 UT. During this time interval from 01:00 UT to 08:00 UT, the count rate from the diffuse ion distribution increases significantly compared to the previous interval and covers a wider angular sector consistent with the diffuse nature of the bow shock accelerated ions.

[24] Between about 08:00 UT and 14:00 UT, the IMF has rotated and the IBEX satellite was not magnetically connected to the bow shock. The distance of the IBEX satellite to the closest magnetic tangent with the bow shock was about $7\,R_E$. IBEX was again connected to the quasi-parallel bow shock between about 14:00 UT and 19:00 UT. During this time interval, the distance to the bow shock has increased to about $15\,R_E$ and the angular coverage of the diffuse ion population is greatly reduced, consistent with expectations.

[25] At about 07:30 UT, the IBaM registered a high count rate event with values in the 20,000 count rate range in all directions (marked with a black arrow in Figure 5 (top))

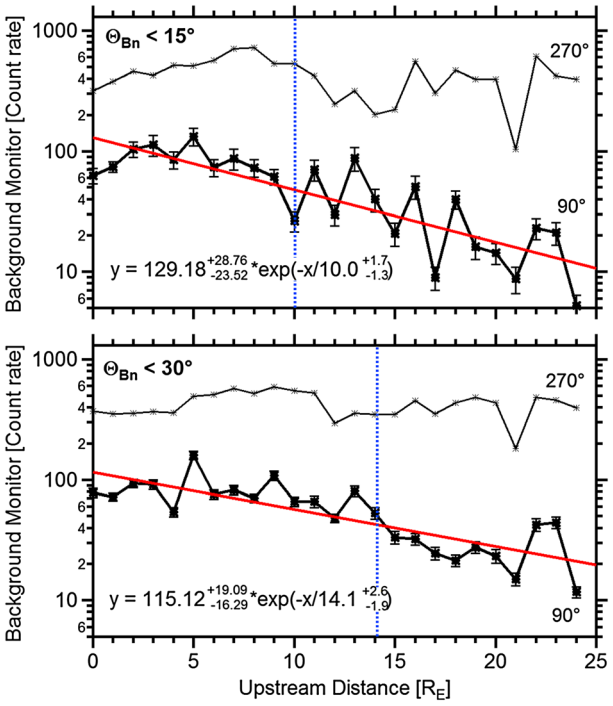

Figure 8. Count rate from the IBEX Background Monitor sectors (resolution 6°) pointing toward and away from the quasi-parallel bow shock at 270° (thin lines) and 90° (thick lines), respectively. The data are plotted versus the IBEX upstream distance along the ambient magnetic field for the bins shown in Figure 7.

caused by penetrating radiation. As shown in Figure 3, this study investigates changes in the count rate of the IBaM sectors away from the bow shock (around 90°), which are usually in the 20 to 40 range. Such omnidirectional but short (one spectrum) count rate spikes as the one at 07:30 UT on 17 February 2009 would completely mask subtle changes in the count rate for the backstreaming diffuse ions and are removed from the data set.

[26] To avoid contamination of the IBaM diffuse ion data by such high count rate omnidirectional events, we processed the data to automatically remove all data points with an average count rate over all sectors > 1000. Additional data selection criteria applied are a magnetic connection from the satellite to the bow shock with a $\Theta_{Bn} < 30°$ (or $< 15°$) and an IBEX position of $Y_{GSE} < -20\,R_E$. The latter selects satellite positions at the dawn sector of the bow shock, which has a significantly higher probability of encountering the quasi-parallel bow shock due to the Parker spiral configuration of the IMF. This satellite position restriction also only considers intervals when the satellite is not connected to the nose of the bow shock, which minimizes any influence of high-energy ion beams emanating from the quasi-perpendicular bow shock in the standard Parker spiral configuration of the IMF.

[27] The final parameter considered for the data selection restricts the data base to events with a solar wind speed 400 km/s. It has been demonstrated earlier that an increase in the solar wind velocity results in harder diffuse ion spectra [*Trattner et al.*, 1994, 2001], which corresponds to a higher count rate in the energy range observed by the IBaM sensor.

[28] Using the high-resolution (3 min) IBaM data set over the time period considered for this study and these selection criteria, we accumulated 3594 and 1005 upstream particle intervals for $\Theta_{Bn} < 30°$ and $\Theta_{Bn} < 15°$, respectively. Figure 6 shows two histograms of all $\Theta_{Bn} < 30°$ and $\Theta_{Bn} < 15°$ intervals considered in this study versus the Alfvén Mach number (M_A). For both histograms, a similar distribution is found that is centered on $M_A = 4$, falls off quickly toward lower Mach numbers, and, for higher Mach numbers, extends to as high as $M_A = 20$.

[29] Figure 7 shows the spin angle distribution of the IBaM count rate versus the IBEX upstream distance from the bow shock along the ambient magnetic field. Color coded in $6° \times 1\,R_E$ bins is the count rate for each spin angle sector for $\Theta_{Bn} < 15°$ (Figure 7, top) and $\Theta_{Bn} < 30°$ (Figure 7, bottom). White areas within the panels show bins with count rates above the maximum count rate used for the color bar. For both panels, the count rate in the IBaM sectors looking toward the bow shock (around 270°) is very stable up to the scan range of 25 R_E upstream from the bow shock. In contrast, the count rate for the sectors in the direction of backstreaming diffuse ions (around 90°) shows a significant variation with upstream distance. For the 3594 intervals with $\Theta_{Bn} < 30°$, the count rate significantly decreases between ~10 and 20 R_E upstream of the bow shock, indicating that there is indeed a decoupling of the diffuse ion population from the upstream wavefield. For the 1005 intervals with $\Theta_{Bn} < 15°$, there is also an observed decrease in the count rate beyond ~10 R_E, but the variation with distance is not as smooth as for the $\Theta_{Bn} < 30°$ cases. For these intervals, some areas further upstream continue to exhibit a higher count rate comparable to regions closer to the bow shock. As will be shown below, the free escape boundaries at about 14 R_E and 10 R_E for the $\Theta_{Bn} < 30°$ and $\Theta_{Bn} < 15°$ surveys, respectively, are the regions where the count rate decreases by about 1/*e* from the count rate closer to the bow shock.

[30] Figure 8 shows the diffuse ion count rate for the IBaM sector toward and away from the bow shock at 270° and 90°, respectively (see Figure 7). The count rate in the 270° sector for both Θ_{Bn} surveys is about constant over the distance surveyed for this study. In contrast, the IBaM sectors for the look direction away from the bow shock, detecting diffuse ions streaming toward the shock (see Figure 4), decrease with increasing distance from the shock. The IBaM sectors at 90° for $\Theta_{Bn} < 30°$ and $\Theta_{Bn} < 15°$ have been fit with exponential functions, with the functions plotted in the two panels of Figure 8. For these backscattered energetic ions, no sharp clearly defined free escape boundary is observed. Rather the decrease is a more gradual decoupling of diffusive ions from the wavefield that scatters them back to the bow shock. The 1/*e* level, marked by a blue dotted line, is reached at a distance of about 14 R_E for the $\Theta_{Bn} < 30°$ distribution (Figure 8, bottom). The distribution of the IBaM count rate for the $\Theta_{Bn} < 15°$ survey (Figure 8, top) is less smooth compared to the $\Theta_{Bn} < 30°$ survey; which might be related to the smaller number of events. The exponential fit of the data drops to 1/*e* at about 10 R_E.

[31] Figure 9 shows the event statistics for the 1 R_E wide upstream distance bins shown in Figure 7. The dashed blue line marks the location of the 1/*e* decrease in the IBaM count rate as determined above, which appears to indicate the existence of a free escape boundary. Figure 9 (top) depicts the

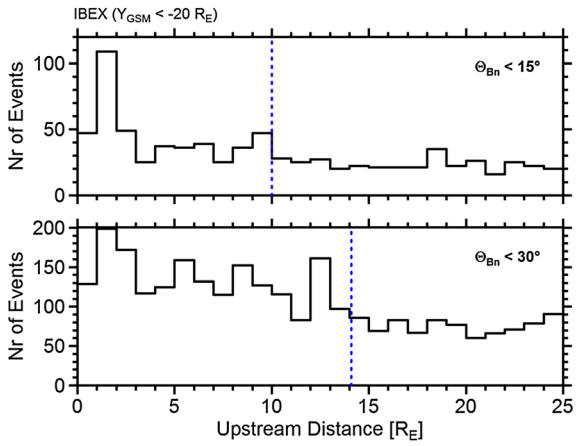

Figure 9. The number of events for the individual upstream distance bins shown in Figure 7. The blue vertical dashed lines indicate the position of the free escape boundary derived above.

number of intervals per upstream distance bin for $\Theta_{Bn} < 15°$. Close to the bow shock, where magnetic connection to an almost parallel shock is easily achieved, the number of intervals per bin peaks at about 120. With increasing distance from the bow shock, this number decreases rapidly and settles around 30 intervals per bin at a distance of 3 R_E, well away from the change in the IBaM counting statistics at about 10 R_E. Beyond the ~10 R_E boundary, the number of intervals per distance bin slowly decreases to around 20.

[32] Figure 9 (bottom) shows the number of intervals per upstream distance bin for $\Theta_{Bn} < 30°$. Since it is easier to connect to the bow shock with a wider Θ_{Bn} range, these numbers are considerably higher. Close to the bow shock, there are about 200 intervals per bin; which slowly decreases for larger distances. The number of intervals up to a distance of 13 R_E is quite variable between the high value of 200 at 1 R_E and about 90 at 11 R_E. Beyond 13 R_E, the number of intervals falls below the 100 per bin level and then settles between 60 and 100. This change in the interval number occurs well away from the change in the IBaM diffuse ion count rate at about 14 R_E.

4. Summary and Conclusion

[33] Models describing energetic diffuse ions upstream of the quasi-parallel bow shock have successfully described features such as their general directional distributions, as well as spectral and spatial distributions in front of the bow shock [e.g., *Ipavich et al.*, 1981a; *Scholer et al.*, 1980b, 1981, 1989; *Trattner et al.*, 1994]. The diffuse ion spectrum upstream of a plane quasi-parallel shock is expected to be a power law independent of the mean free path of the diffuse ions under stationary conditions. The observed spectra at the spatially limited Earth's bow shock deviate from a simple power law and can be best described by an exponential function in energy per charge above 30 keV/*e* [*Ipavich et al.*, 1981a].

[34] Models account for this deviation by including additional assumptions, e.g., a finite time of magnetic connection for diffuse ions with the bow shock [*Scholer et al.*, 1980a; *Forman and Drury*, 1983] or the loss of ions due to diffusion perpendicular to the magnetic field [e.g., *Lee*, 1982]. Models also use ion loss across a free escape boundary along the interplanetary magnetic field into the upstream direction [e.g., *Ellison*, 1981; *Lee et al.*, 1981]. In shock simulation studies, such a free escape boundary is a natural consequence of the finite size of the simulation system and is therefore artificial. However, the free escape boundary has also been used deliberately at a fixed distance upstream of the shock to simulate the observed diffuse ion spectra with Monte Carlo methods [e.g., *Ellison and Möbius*, 1987; *Ellison et al.*, 1990]. However, this concept is also supported by simultaneous observation of energetic ions at ISEE 3 more than 200 R_E upstream and ISEE 1 close to the quasi-parallel bow shock, respectively [*Scholer et al.*, 1980b]. ISEE 1 and ISEE 3 both observed energetic ion distributions when they were magnetically connected with the quasi-parallel bow shock. While the ion distribution close to the bow shock was more or less isotropic, indicating strong scattering of the ions in the upstream wavefield, the ion distribution far upstream moved essentially scatter free away from the bow shock. Somewhere in the upstream region of a quasi-parallel shock, shock-accelerated diffuse ions decouple from the acceleration region and stream away, which lets them escape from the region where Fermi acceleration is effective.

[35] With the IBEX satellite, we cover for the first time the region upstream of the shock where the decoupling of energetic shock-accelerated ions from the upstream wavefield is thought to take place. For this investigation, we use the IBEX Background Monitor with a time resolution of 3 min. The IBaM is sensitive to energetic ions above 14 keV with a 7° FWHM FOV. Two different surveys at $\Theta_{Bn} < 15°$ and $\Theta_{Bn} < 30°$ have been undertaken for this study. Several selection criteria have been used in assembling the data base. Omnidirectional spikes in the count rate of the IBaM prompted rejection of all intervals where the average count rate over all sectors exceeds 1000. Only IBEX positions with $Y_{GSE} < -20\,R_E$ are considered in the survey to focus on the dawnside of the magnetosphere where the quasi-parallel bow shock is more common due to the Parker spiral configuration of the IMF. Finally, only solar wind intervals with a solar wind velocity $V > 400$ km/s are considered since higher solar wind velocities cause harder diffuse ion spectra and higher count rates in the IBaM. These selection criteria result in 3594 and 1005 upstream particle intervals for $\Theta_{Bn} < 30°$ and $\Theta_{Bn} < 15°$, respectively.

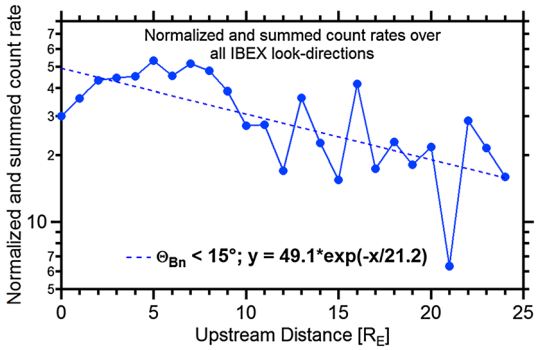

Figure 10. Count rate from the IBEX Background Monitor sectors normalized and summed over all look directions. The data are plotted versus the IBEX upstream distance along the ambient magnetic field for the bins shown in Figure 7.

[36] Count rates in the IBaM sector looking along the ambient magnetic field direction toward the bow shock are constant for the upstream scanning range from 0 to 25 R_E. In contrast, the count rate for the IBaM sector looking away from the shock and detecting diffuse ions scattered back in the ambient upstream wavefield shows a gradual decrease with increasing distance from the bow shock. The count rate decreases by $1/e$ at 10 R_E and 14 R_E for $\Theta_{Bn} < 15°$ and $\Theta_{Bn} < 30°$, respectively. A distinct free escape boundary does not really exist in nature because of the gradual decay of wave activity upstream of the shock. The concept of a free escape boundary upstream of the Earth's bow shock is thought to be a limitation of the upstream wavefield to some distance close to the shock which seems to be located around 14 R_E. The gradual decrease of the backscattered diffuse ions indicates a gradual decoupling of the diffuse ions from the upstream wavefield and thus supports that concept. It also shows that this boundary, for which we adopt the definition that the relevant particle fluxes are reduced to $1/e$ of the original levels, is rather a gradual transition.

[37] As mentioned above, the IBaM instrument makes integral measurements of protons above an energy of ~14 keV which makes it impossible to investigate an energy dependence of such a free escape boundary with this instrument. An energy dependence of the boundary is expected since the upstream diffusion coefficient generally depends on energy, and therefore, the *e*-folding distance describing the spatial dependence of the energetic ion flux upstream along the magnetic field also depends on energy. This dependency was described in a statistical study with AMPTE/IRM observations that showed that the *e*-folding distance for diffuse ions increases with energy from about 3.2 R_E at 10 keV to 9.3 R_E at 67.3 keV [*Trattner et al*., 1994]. Similar results were reported by *Ipavich et al*. [1981a] using ISEE data. They found *e*-folding distances of 7 R_E and 8 R_E for 30 and 65 keV/*e* protons. *Kronberg et al*. [2009], using Cluster observations, also found *e*-folding distances of about 6.5 R_E and 16 R_E for 42 and 123 keV/*e* protons, respectively. A study by *Kis et al*. [2004] using simultaneous multipoint observations by the Cluster satellite in the energy range from 10 to 32 keV found *e*-folding distances of about half the values reported earlier by *Ipavich et al*. [1981a] and *Trattner et al*. [1994]. Consistent with these previous studies and shock acceleration theory, the normalized averaged IBaM data used in this study also exhibit a spatial gradient upstream of the bow shock with an *e*-folding distance of about 21 R_E (Figure 10). However, this *e*-folding distance cannot be directly compared to previous measurements of spatial gradients since the IBaM is not a true omnidirectional instrument but only observes a 7° swath of the upstream distribution (see Figure 4). As shown in Figure 8, not all angular sectors of the diffuse ion distribution have the same spatial gradients. Energetic ions streaming away from the bow shock exhibit no significant spatial gradient compared to energetic ions streaming toward the bow shock. This result has been confirmed with Cluster observations (E. Kronberg, personal communications, 2013).

[38] Fluxes of shock-accelerated ions with higher energies have smaller spatial gradients in the upstream direction than accelerated ions with lower energies and should exhibit their own energy-dependent free escape boundaries. The gradual decrease of the backscattered diffuse ions and the related upstream wave activity together with the expected energy dependency suggests that this phenomenon is better described as a free escape continuum, which would replace the rigid free escape boundary concept.

[39] **Acknowledgments.** We acknowledge the use of ISTP KP database. Solar wind observations were provided by the ACE Solar Wind Experiment (ACE/SWE) [*McComas et al*., 1998]. The IMF measurements are provided by the ACE Magnetic Field Instrument (ACE/MFI) [*Smith et al*., 1998]. Support for this study comes from the IBEX mission as a part of NASA's Explorer program. IBEX is the result of efforts from a large number of scientists, engineers, and others; all who contributed to this mission share in its success. The work at Lockheed Martin was supported by NASA contracts 599769Q, NNX08AF35G, NNX09AM72G, NNX11AJ09G, and NNG05GE15G and by grant 1102572 from the National Science Foundation.

[40] Philippa Browning thanks the reviewers for their assistance in evaluating this paper.

References

Allegrini, F., G. B. Crew, D. Demkee, H. O. Funsten, D. J. McComas, B. Randol, B. Rodriguez, N. A. Schwadron, P. Valek, and S. Weidner (2009), The IBEX Background Monitor, *Space Sci. Rev.*, *146*(1), 105–115.

Asbridge, J. R., S. J. Bame, and I. B. Strong (1968), Outward flow of protons from the Earth's bow shock, *J. Geophys. Res.*, *73*, 5777–5782.

Axford, W.I., E. Leer, and G. Skadron (1977), The acceleration of cosmic rays by shock waves, in *Proc. 15th Int. Cosmic Rays Conf*., vol. *11*, Bulgaria, August 13–26, 132 pp., Max Planck Institut fuer Aeronomie, Katlenburg-Lindau, Germany.

Bonifazi, C., and G. Moreno (1981), Reflected and diffuse ions backstreaming from the Earth's bow shock, *J. Geophys. Res.*, *86*, 4397–4404.

Ellison, D. C. (1981), Monte Carlo simulation of charged particles upstream of the Earth's bow shock, *Geophys. Res. Lett.*, *8*, 991–994.

Ellison, D. C., and E. Möbius (1987), Diffusive shock acceleration: Comparison of a unified shock model to bow shock observations, *Astrophys. J.*, *318*, 474–484.

Ellison, D. C., E. Möbius, and G. Paschmann (1990), Particles injection and acceleration at Earth's bow shock: Comparison of upstream and downstream events, *Astrophys. J.*, *352*, 376–394.

Fairfield, D. H. (1969), Bow shock associated waves observed in the far upstream interplanetary medium, *J. Geophys. Res.*, *74*, 3541–3553.

Farris, M. H., and C. T. Russell (1994), Determining the standoff distance of the bow shock: Mach number dependence and use of models, *J. Geophys. Res.*, *99*, 17,681–17,689.

Forman, M. A., and L.O. Drury (1983), Time dependent shock acceleration: Approximations and exact solutions, *Conf. Pap. Int. Cosmic Ray Conf.* 18th, OG 6–16, pp. 267–270.

Funsten, H. O., et al. (2009), The Interstellar Boundary Explorer High Energy (IBEX-Hi) Neutral Atom Imager, *Space Sci. Rev.*, *146*, 103–75, doi:10.1007/s11214-009-9504-y.

Gordon, B. E., M. A. Lee, E. Möbius, and K. J. Trattner (1999), Coupled hydromagnetic wave excitation and ion acceleration at interplanetary traveling shocks and the Earth's bow shock, *J. Geophys. Res.*, *104*, 28,263–28,277.

Gosling, J. T., J. R. Asbridge, S. J. Bame, G. Paschmann, and N. Sckopke (1978), Observations of two distinct populations of bow shock ions in the upstream solar wind, *Geophys. Res. Lett.*, *5*, 957–960.

Greenstadt, E. W. (1976), Phenomenology of the Earth's bow shock system: A summary description of experimental results, in *Magnetospheric Particles and Fields*, edited by M. McCormac, pp.13–28, D. Reidel Hingham, Mass.

Hoppe, M. M., C. T. Russell, L. A. Frank, T. E. Eastman, and E. W. Greenstadt (1981), Upstream hydromagnetic waves and their association with backstreaming ions populations: ISEE-1 and ISEE-2 observations, *J. Geophys. Res.*, *86*, 4471–4492.

Ipavich, F. M., A. B. Galvin, G. Gloeckler, M. Scholer, and D. Hovestadt (1981a), A statistical survey of ions observed upstream of the Earth's bow shock: Energy spectra, composition and spatial variations, *J. Geophys. Res.*, *86*, 4337–4342.

Ipavich, F. M., M. Scholer, and G. Gloeckler (1981b), Temporal development of composition, spectra and anisotropies during upstream particle events, *J. Geophys. Res.*, *86*, 11,153–11,160.

Jokipii, J. R. (1982), Particle drift, diffusion and acceleration at shocks, *Astrophys. J.*, *255*, 716–720.

Kis, A., M. Scholer, B. Klecker, E. Möbius, E. A. Lucek, H. Reme, J. M. Bosqued, L. M. Kistler, and H. Kucharek (2004), Multi-spacecraft observations of diffuse ions upstream of Earth's bow shock, *Geophys. Res. Lett.*, *31*, L20801, doi:10.1029/2004GL020759.

Krimigis, S. M., D. Venkatesan, J. C. Barichello, and E. T. Sarris (1978), Simultaneous measurements of energetic protons and electrons in the distant magnetosheath, magnetotail and upstream in the solar wind, *Geophys. Res. Lett.*, *5*, 961–964.

Kronberg, E. A., A. Kis, B. Klecker, P. W. Daly, and E. A. Lucek (2009), Multipoint observations of ions in the 30–160 keV energy range upstream of the Earth's bow shock, *J. Geophys. Res.*, *114*, A03211, doi:10.1029/2008JA013754.

Lee, M. A. (1982), Coupled hydromagnetic wave excitation and ion acceleration upstreams of the Earth's bow shock, *J. Geophys. Res.*, *87*, 5063–5080.

Lee, M. A., G. Skadron, and L. A. Fisk (1981), Acceleration of energetic ions at the Earth's bow shock, *Geophys. Res. Lett.*, *8*, 401–404.

Lin, R. P., C. I. Meng, and K. A. Anderson (1974), 30 to 100 keV protons upstream from the Earth's bow shock, *J. Geophys. Res.*, *79*, 489–498.

McComas, D. J., S. J. Bame, P. Barker, W. C. Feldman, J. L. Phillips, P. Riley, and J. W. Griffee (1998), Solar Wind Electron Proton Alpha Monitor (SWEPAM) for the Advanced Composition Explorer, *Space Sci. Rev.*, *86*, 563–612.

McComas, D. J., et al. (2009a), IBEX—Interstellar Boundary Explorer, *Space Sci. Rev.*, *146*, 11–33, doi:10.1007/s11214-009-9499-4.

McComas, D. J., et al. (2009b), Global observations of the interstellar interaction from the Interstellar Boundary Explorer (IBEX), *Science*, *326*, 959–962, doi:10.1126/science.1180906.

Möbius, E., M. Scholer, N. Skopke, H. Lühr, G. Paschmann, and D. Hovestadt (1987), The distribution function of diffuse ions and the magnetic field power spectrum upstream of the Earth's bow shock, *Geophys. Res. Lett.*, *14*, 681–684.

Paschmann, G., N. Sckopke, I. Papamastorakis, J. R. Asbridge, S. J. Bame, and J. T. Gosling (1981), Characteristics of reflected and diffuse ions upstream from the Earth's bow shock, *J. Geophys. Res.*, *86*, 4355–4364.

Petrinec, S. M., and C. T. Russell (1996), Near-Earth magnetotail shape and size as determined from the magnetopause flaring angle, *J. Geophys. Res.*, *101*, 137–152.

Sarris, E. T., S. M. Krimigis, and T. P. Armstrong (1976), Observation of magnetospheric bursts of high-energy protons and electrons at ~35 R_E with IMP 7, *J. Geophys. Res.*, *81*, 2341–2355.

Sarris, E. T., S. M. Krimigis, C. O. Bostrom, and T. P. Armstrong (1978), Simultaneous multispacecraft observations of energetic proton bursts inside and outside the magnetosphere, *J. Geophys. Res.*, *83*, 4289.

Scholer, M., G. Gloeckler, F. M. Ipavich, P. Hovestadt, and B. Klecker (1979), Pitch angle distributions of energetic protons near the Earth's bow shock, *Geophys. Res. Lett.*, *6*, 707–710.

Scholer, M., F. M. Ipavich, G. Gloeckler, and D. Hovestadt (1980a), Conditions for acceleration of energetic ions >30 keV associated with the Earth's bow shock, *J. Geophys. Res.*, *85*, 4602–4606.

Scholer, M., F. M. Ipavich, G. Gloeckler, D. Hovestadt, and B. Klecker (1980b), Upstream particle events close to the bow shock and 200 R_E upstream: ISEE-1 and ISEE-3 observations, *Geophys. Res. Lett.*, *7*, 73–76.

Scholer, M., F. M. Ipavich, and G. Gloeckler (1981), Beams of protons and alpha particles >30 keV/charge from the Earth's bow shock, *J. Geophys. Res.*, *86*, 4374–4378.

Scholer, M., E. Möbius, L. M. Kistler, and B. Klecker (1989), Multispacecraft observations of energetic ions upstream and downstream of the bow shock, *Geophys. Res. Lett.*, *16*, 571–574.

Smith, C. W., M. H. Acuna, L. F. Burlaga, J. L'Heureux, N. F. Ness, and J. Scheifele (1998), The ACE magnetic field experiment, *Space Sci. Rev.*, *86*, 613–632.

Trattner, K. J., E. Möbius, M. Scholer, B. Klecker, M. Hilchenbach, and H. Lühr (1994), Statistical analysis of diffuse ion events upstream of the Earth's bow shock, *J. Geophys. Res.*, *99*, 13,389–13,400.

Trattner, K. J., S. A. Fuselier, W. K. Peterson, S.-W. Chang, R. Friedel, and M. R. Aellig (2001), Origins of energetic ions in the cusp, *J. Geophys. Res.*, *106*, 5967–5976.

Wurz, P., et al. (2009), IBEX backgrounds and signal-to-noise ratio, *Space Sci. Rev.*, *146*, 173–206.